Supporting Information

Mixed-Substituted Single-Source Precursors for $Si_{1-x}Ge_x$ Thin Film Deposition

Benedikt Köstler,[1] Felix Jungwirth,[2] Luisa Achenbach,[1] Masiar Sistani,[3] Michael Bolte,[1] Hans-Wolfram Lerner,[1] Philipp Albert,[4] Matthias Wagner,[1,] and Sven Barth[2,*]*

[1] Institute for Inorganic and Analytical Chemistry, Goethe University Frankfurt, Max-von-Laue-Str. 7, 60438 Frankfurt, Germany.

[2] Physical Institute, Goethe University Frankfurt, Max-von-Laue-Str. 1, 60438 Frankfurt, Germany.

[3] Institute of Solid State Electronics, TU Wien, Gußhausstraße 25-25a, 1040 Vienna, Austria.

[4] Evonik Operations GmbH, Smart Materials, Untere Kanalstraße 3, 79618 Rheinfelden, Germany.

Corresponding authors:

M. Wagner: matthias.wagner@chemie.uni-frankfurt.de

S. Barth: barth@physik.uni-frankfurt.de

Content:

1. Proposed Process for the Formation of the Si–Ge precursors

A) Generation of trichlorosilanide *via* the Cl^--induced disproportionation of Si_2Cl_6

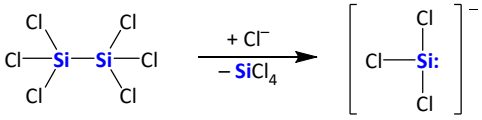

B) Generation of diphenyl(chloro)germanide *via* Cl^+-ion abstraction

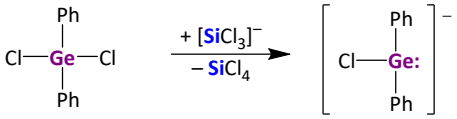

B_1) Known formation of isolable trichlorogermanide

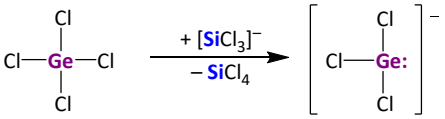

C) Germanide attacks Ph_2GeCl_2 to build a Ge-Ge bond; digermane is silylated twice to form **1-Cl**

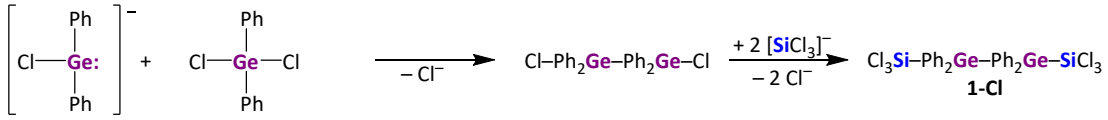

D) Germanide attacks Si_2Cl_6 to build a Ge-Si bond; silylgermane is silylated again to form **2-Cl**

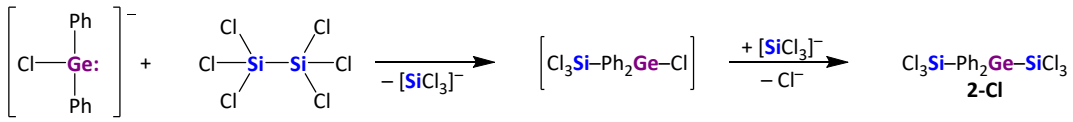

=> Theoretically required stoichiometries according to the proposed mechanism

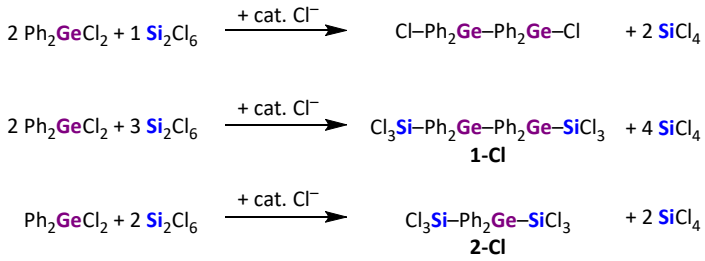

Experimentally optimized stoichiometries

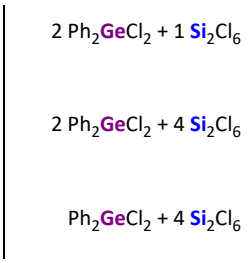

Figure S1. Conceivable mechanism to rationalize the stoichiometries *n*:*m* required for the formation of **1-Cl** and **2-Cl** from *n* Ph_2GeCl_2, *m* Si_2Cl_6, and cat. [*n*Bu_4N]Cl; for B_1, see Ref.[1]

A) The Cl^--induced heterolysis of the Si–Si bond in Si_2Cl_6 leads to the formation of $SiCl_4$ and the reactive intermediate $[SiCl_3]^-$.[2]

B) $[SiCl_3]^-$ abstracts a Cl^+ ion from Ph_2GeCl_2 to generate $[Ph_2GeCl]^-$ and $SiCl_4$. This assumption is supported by the known reaction of $GeCl_4$ with $[SiCl_3]^-$, which yields $SiCl_4$ and the isolable germanide $[GeCl_3]^-$ (cf. **B_1**).[1] Although $[GeCl_3]^-$ itself is a very weak nucleophile, its Ph derivatives have been successfully employed to generate digermanes, e.g., Ph_3GeNa +

Et_3GeBr → $Ph_3Ge–GeEt_3$ + NaBr.[3, 4] Given this background, it is reasonable to assume that also $[Ph_2GeCl]^-$ is sufficiently nucleophilic to attack either the Ge atom in Ph_2GeCl_2 (cf. **C**) or the Si atoms in Si_2Cl_6 or $SiCl_4$ (cf. **D**). These two pathways compete with each other.

C) We have shown by experiment that the reaction of 2 Ph_2GeCl_2 with 1 Si_2Cl_6 and cat. [*n*Bu_4N]Cl affords Cl–Ph_2Ge–Ph_2Ge–Cl as main product ($^{13}C\{^1H\}$ NMR spectroscopic control; isolated in 43% yield). Subsequent treatment of the digermane with 2 Si_2Cl_6/cat. Cl^- indeed furnished **1-Cl**, thereby confirming the proposed reaction mechanism. Although 1.5 equiv. Si_2Cl_6 should be sufficient for the one-pot reaction to **1-Cl**, in practice it is advantageous to use 2 equiv. Si_2Cl_6.

D) First, we have shown by experiment that **1-Cl** is inert toward $[SiCl_3]^-$ under the conditions applied in the synthesis of **2-Cl**. This rules out the digermane **1-Cl** as an intermediate along the path to **2-Cl**, but rather suggests that both Ge–Si bonds are formed already on the monogermane. According to our empirical findings, the theoretically required 2 equiv. Si_2Cl_6 are not sufficient for the formation of **2-Cl**, but rather give **1-Cl**. The problem is solved by use of 4 equiv. Si_2Cl_6 and we believe that the excess is necessary to ensure that Ge–Si-bond formation can outcompete the apparently very favorable Ge–Ge-bond formation.

2. Single-Crystal X-ray Analyses

Data sets for both structures were collected on a STOE IPDS II two-circle diffractometer with a Genix Microfocus tube with mirror optics using MoK_α radiation (λ = 0.71073 Å). The data sets were scaled using the frame-scaling procedure in the *X-AREA* program system.[5] The structures were solved by direct methods using the program *SHELXS*[6] and refined against F^2 with full-matrix least-squares techniques using the program *SHELXL*[6].

CCDC files CCDC 2182827 (**1-Cl**) and CCDC 2182828 (**1-H**) contain the supplementary crystallographic data for this paper and can be obtained free of charge from The Cambridge Crystallographic Data Centre via www.ccdc.cam.ac.uk/data_request/cif.

1-H crystallizes with two half molecules in the asymmetric unit. The other half of both molecules is generated by a two-fold rotation axis. One molecule is shown in Figure 1 of the main article. In the second molecule, the Ge atom and one SiH_3 group are disordered over two equally occupied positions. The absolute structure was determined, Flack-x-parameter 0.06(4).

Table S1. Crystal data and structure refinement for **1-Cl**.

CCDC code	2182827	
Empirical formula	C_{24} H_{20} Cl_6 Ge_2 Si_2	
Formula weight	722.46	
Temperature	173(2) K	
Wavelength	0.71073 Å	
Crystal system	Monoclinic	
Space group	*C2/c*	
Unit cell dimensions	a = 9.8305(5) Å	α = 90°
	b = 17.8639(7) Å	β = 101.309(4)°
	c = 16.8410(9) Å	γ = 90°
Volume	2900.0(2) Å^3	
Z	4	
Density (calculated)	1.655 Mg/m^3	
Absorption coefficient	2.722 mm^{-1}	
F(000)	1432	
Crystal size	0.250 × 0.200 × 0.200 mm^3	
Theta range for data collection	3.729 to 33.205°	
Index ranges	–15<=h<=15, –27<=k<=27, –25<=l<=24	
Reflections collected	33798	
Independent reflections	5510 [R(int) = 0.0864]	
Completeness to theta = 25.000°	99.2 %	
Absorption correction	Semi-empirical from equivalents	
Max. and min. transmission	1.000 and 0.598	
Refinement method	Full-matrix least-squares on F^2	
Data / restraints / parameters	5510 / 0 / 154	
Goodness-of-fit on F^2	0.981	
Final R indices [I>2sigma(I)]	$R1$ = 0.0409, $wR2$ = 0.1014	
R indices (all data)	$R1$ = 0.0475, $wR2$ = 0.1060	
Largest diff. peak and hole	1.333 and –0.643 e·Å^{-3}	

Symmetry transformation used to generate equivalent atoms:–x+1, y, –z+3/2

Table S2. Crystal data and structure refinement for **1-H**.

CCDC code	2182828	
Empirical formula	C_{24} H_{26} Ge_2 Si_2	
Formula weight	515.81	
Temperature	173(2) K	
Wavelength	0.71073 Å	
Crystal system	Monoclinic	
Space group	*C2*	
Unit cell dimensions	a = 16.771(4) Å	α = 90°
	b = 11.529(2) Å	β = 110.932(18)°
	c = 13.476(3) Å	γ = 90°
Volume	2433.7(9) Å^3	
Z	4	
Density (calculated)	1.408 Mg/m^3	
Absorption coefficient	2.576 mm^{-1}	
F(000)	1048	
Crystal size	0.180 × 0.150 × 0.120 mm^3	
Theta range for data collection	3.351 to 26.440°	
Index ranges	–20<=h<=20, –14<=k<=14, –16<=l<=16	
Reflections collected	12091	
Independent reflections	4965 [R(int) = 0.0747]	
Completeness to theta = 25.000°	99.6 %	
Absorption correction	Semi-empirical from equivalents	
Max. and min. transmission	1.000 and 0.750	
Refinement method	Full-matrix least-squares on F^2	
Data / restraints / parameters	4965 / 37 / 267	
Goodness-of-fit on F^2	1.077	
Final R indices [I>2sigma(I)]	*R1* = 0.0842, *wR2* = 0.2128	
R indices (all data)	*R1* = 0.0898, *wR2* = 0.2174	
Largest diff. peak and hole	1.112 and –1.034 e·Å^{-3}	

Symmetry transformation used to generate equivalent atoms: –x+1, y+2, –z+1

3. Plots of ^{1}H, $^{13}C\{^{1}H\}$, $^{29}Si\{^{1}H\}$, and ^{29}Si NMR Spectra

3.1. NMR Spectra of 1-Cl

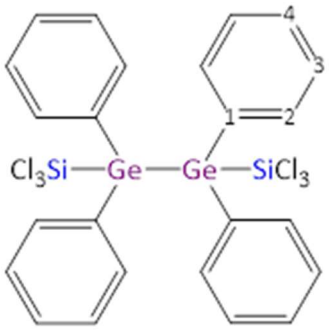

1-Cl

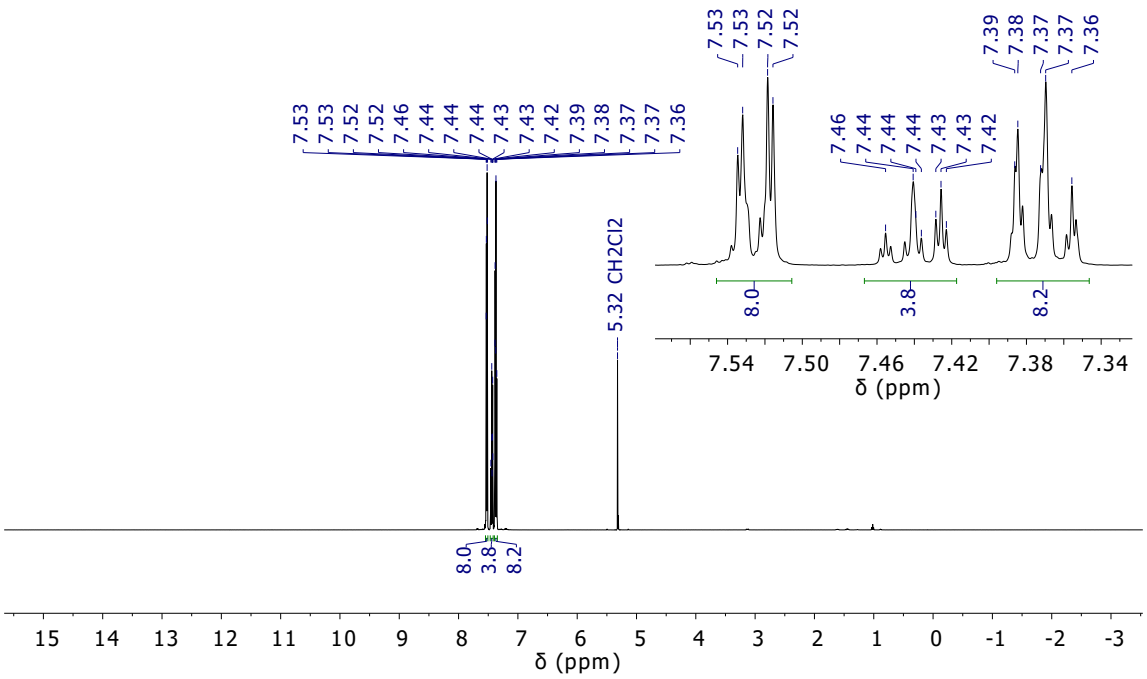

Figure S2. ^{1}H NMR spectrum of **1-Cl** (CD_2Cl_2, 500.2 MHz).

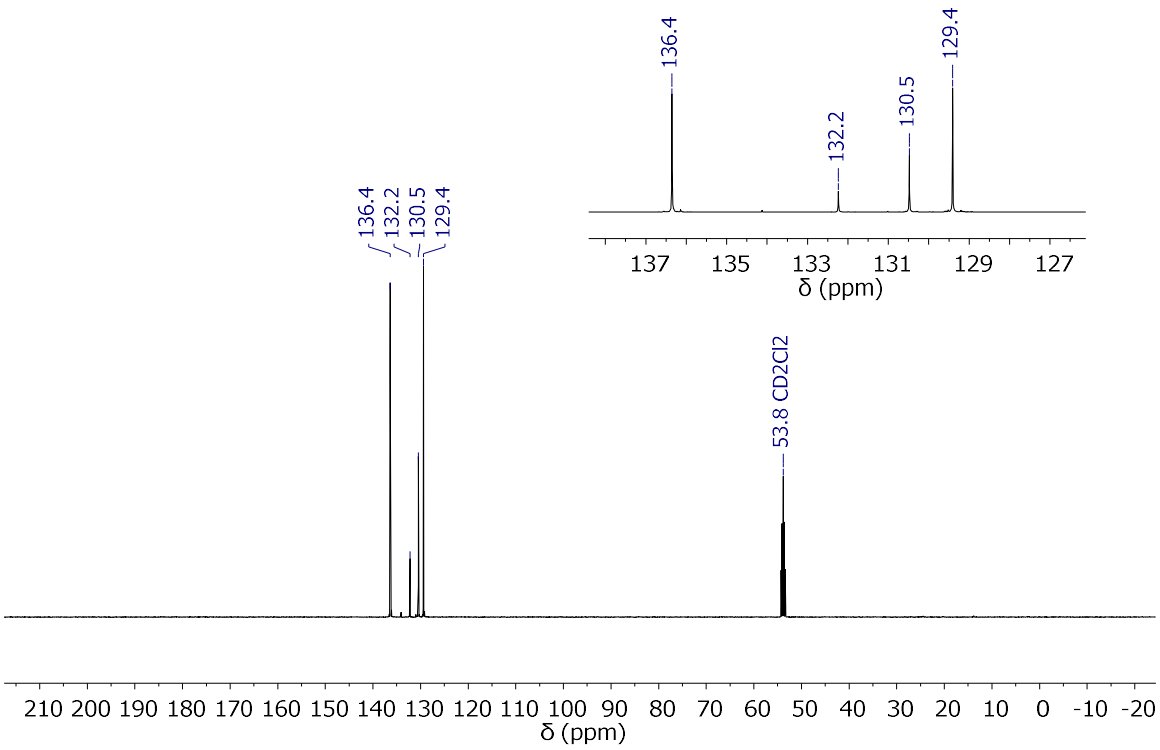

Figure S3. $^{13}C\{^{1}H\}$ NMR spectrum of **1-Cl** (CD_2Cl_2, 125.8 MHz).

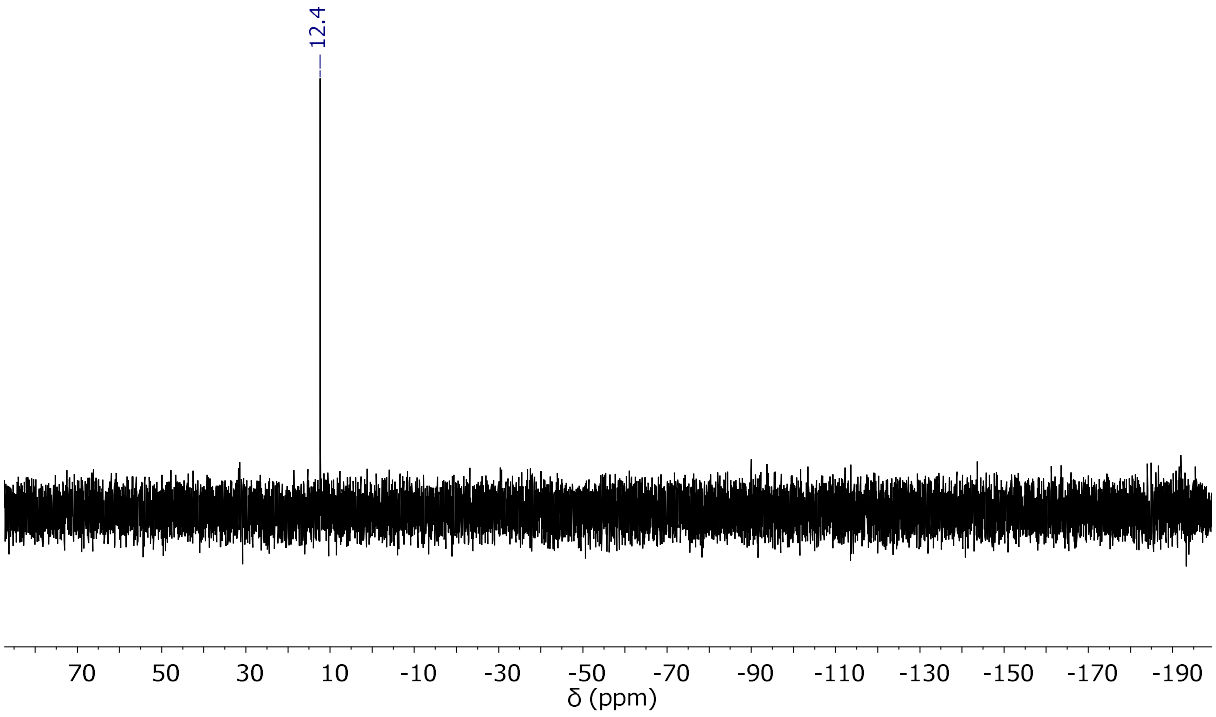

Figure S4. $^{29}Si\{^{1}H\}$ NMR spectrum of **1-Cl** (CD_2Cl_2, 99.4 MHz).

3.2. NMR Spectra of 2-Cl

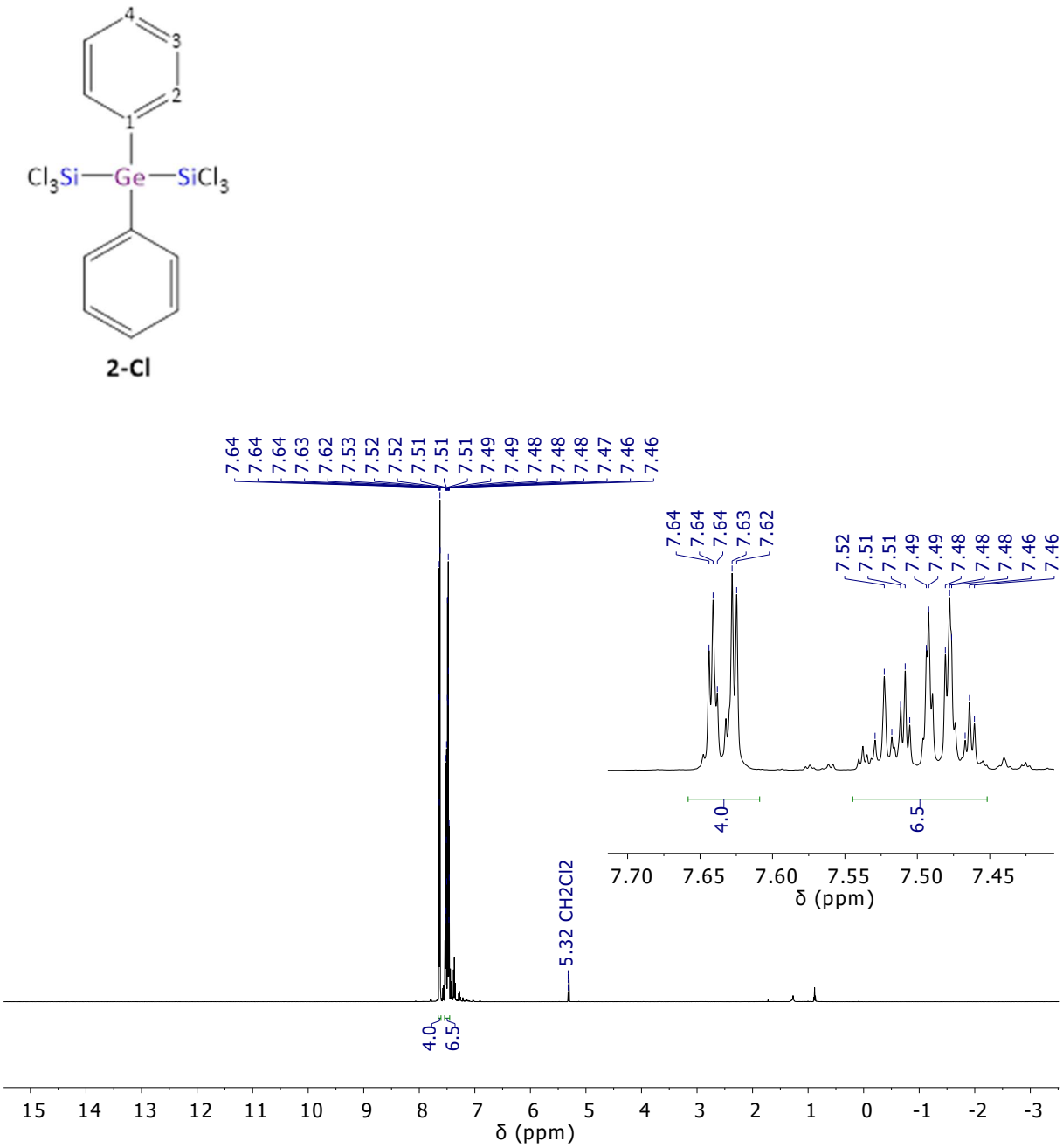

Figure S5. ^{1}H NMR spectrum of **2-Cl** (CD_2Cl_2, 500.2 MHz).

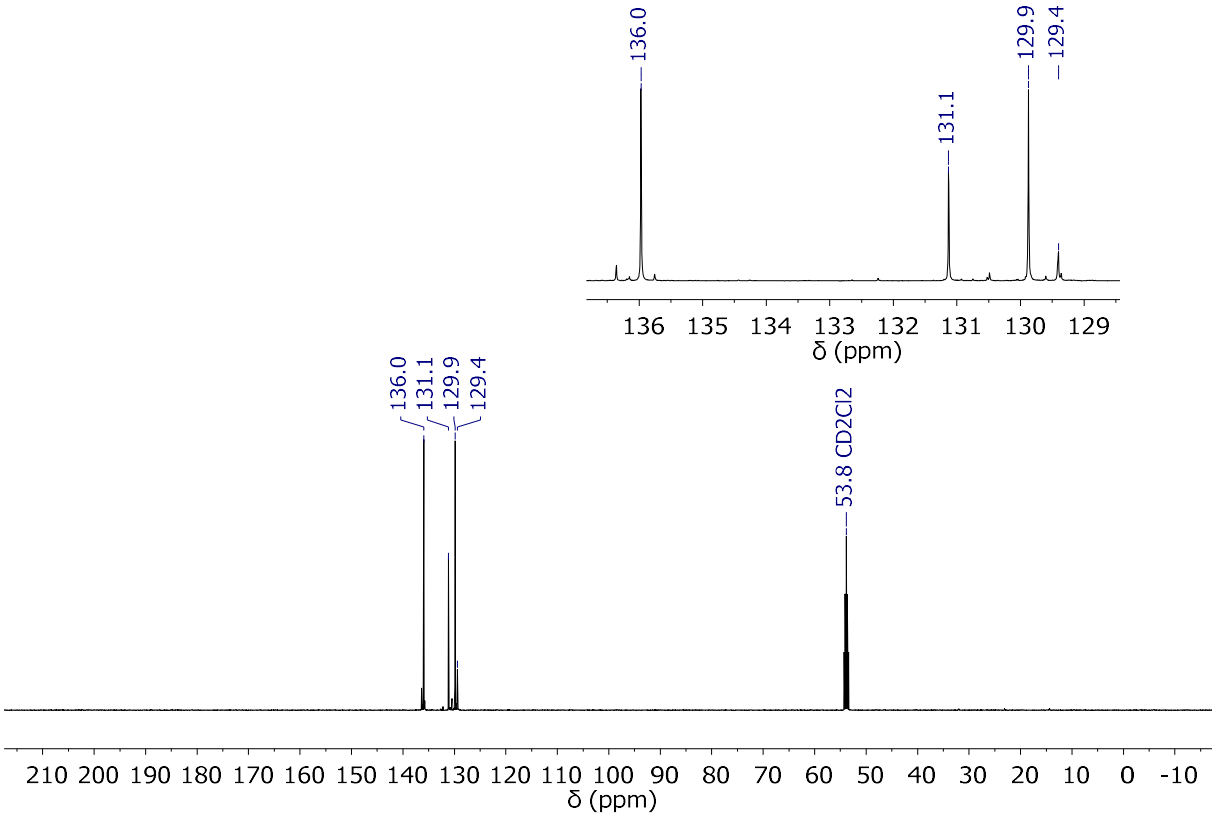

Figure S6. $^{13}C\{^{1}H\}$ NMR spectrum of **2-Cl** (CD_2Cl_2, 125.8 MHz).

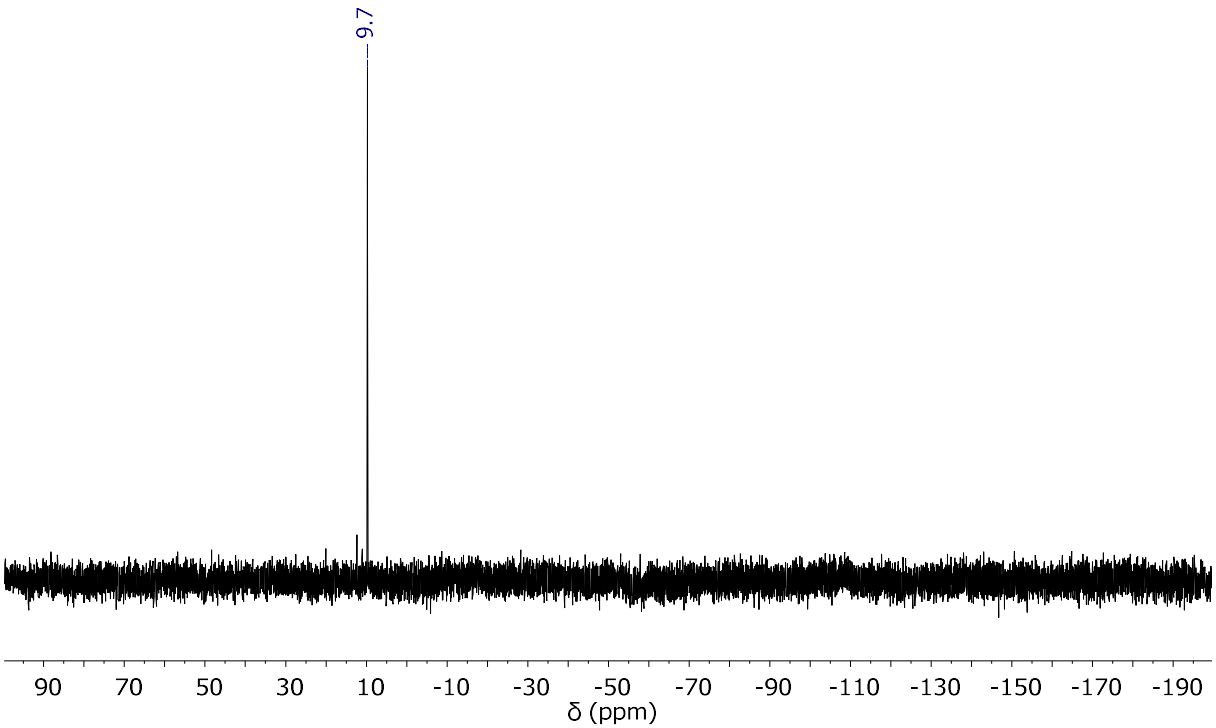

Figure S7. $^{29}Si\{^{1}H\}$ NMR spectrum of **2-Cl** (CD_2Cl_2, 99.4 MHz).

3.3. NMR Spectra of 3-Cl

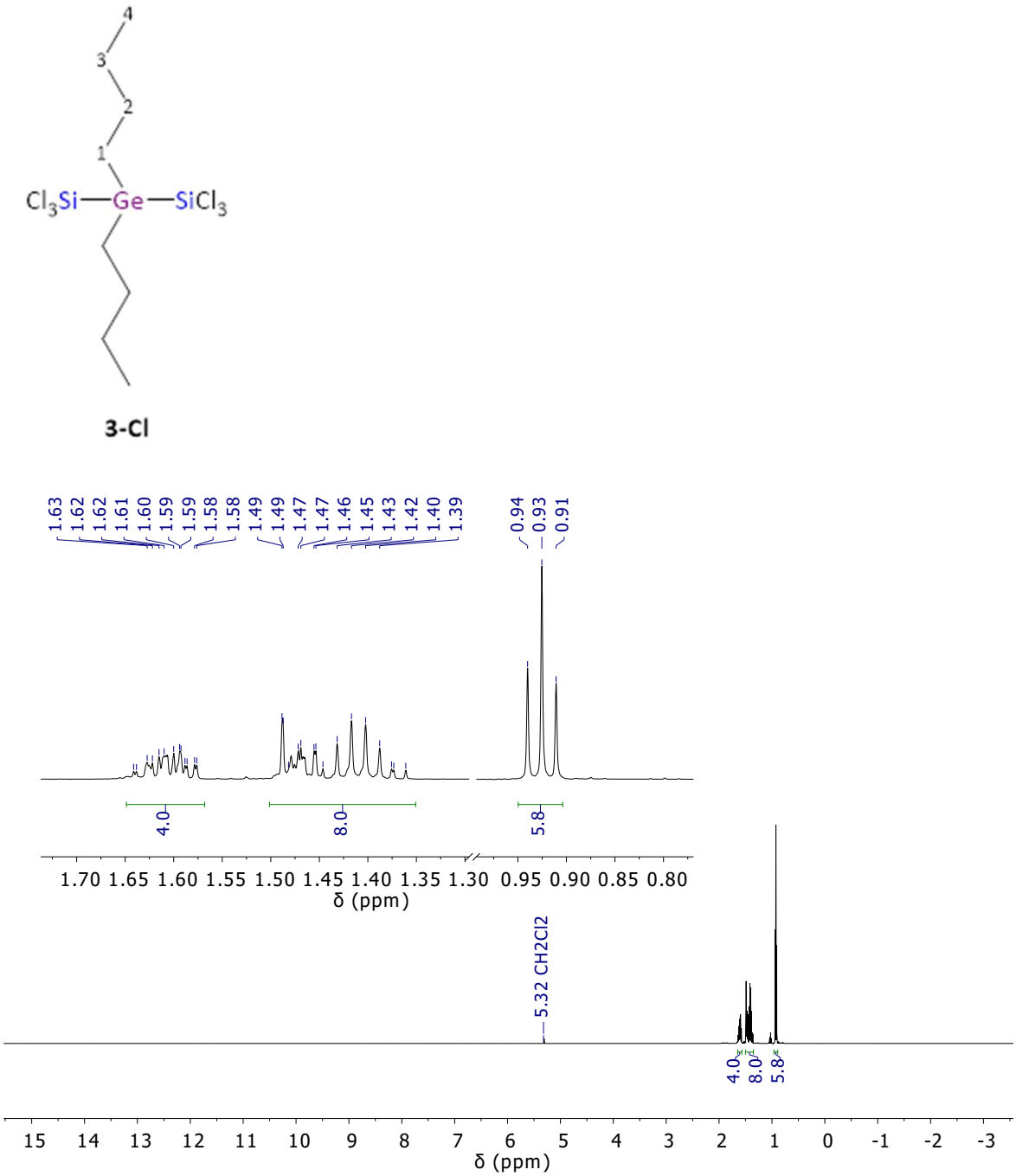

Figure S8. ^{1}H NMR spectrum of **3-Cl** (CD_2Cl_2, 500.2 MHz).

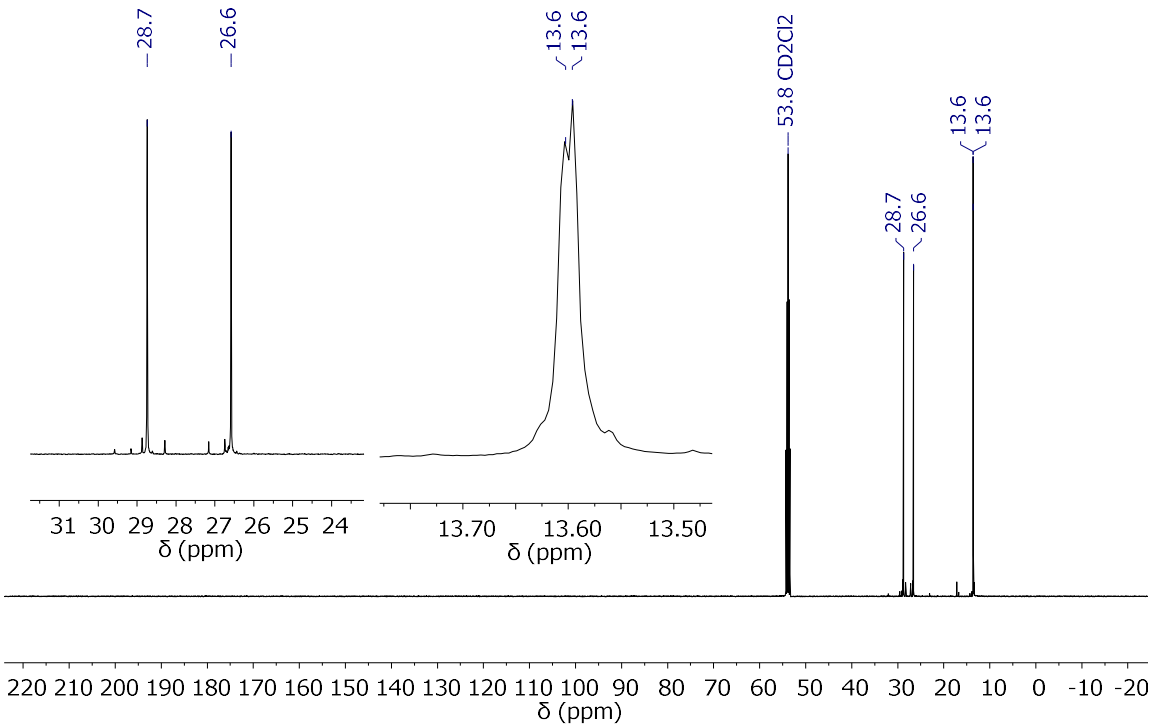

Figure S9. $^{13}C\{^{1}H\}$ NMR spectrum of **3-Cl** (CD_2Cl_2, 125.8 MHz).

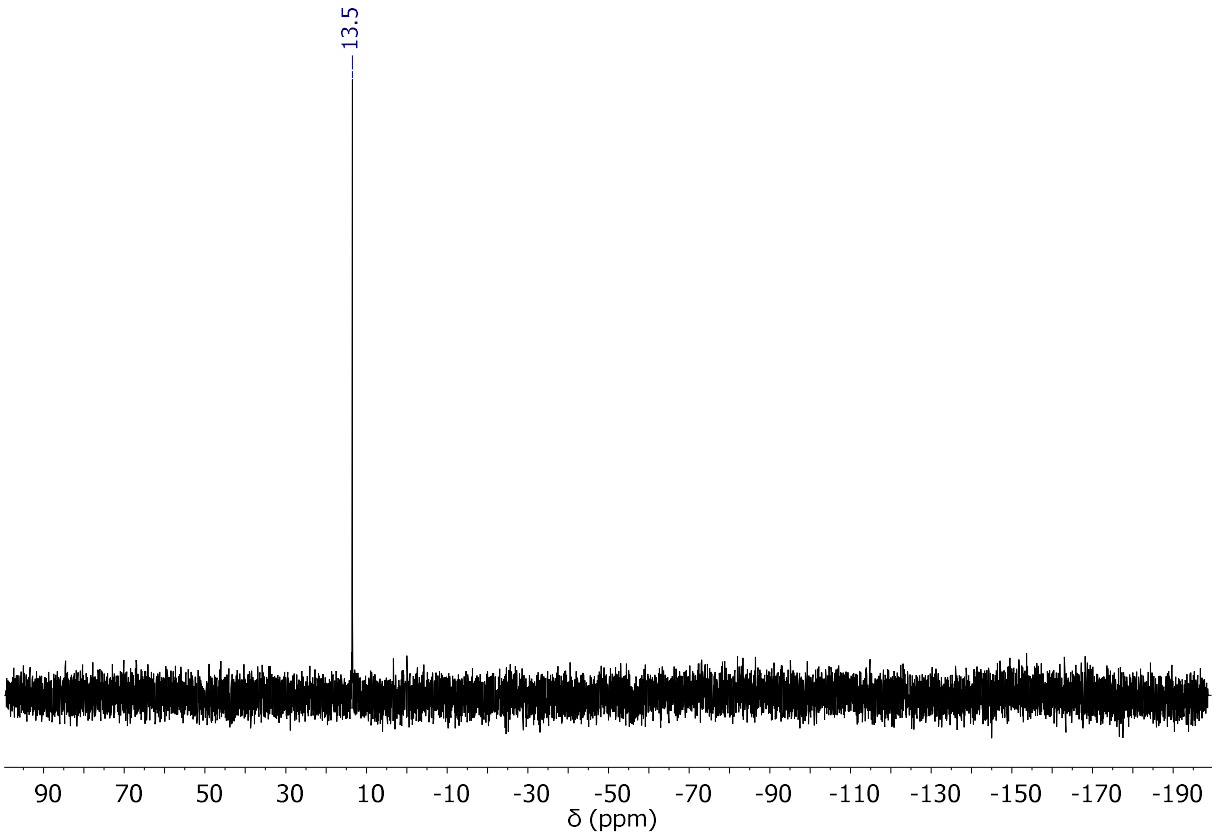

Figure S10. $^{29}Si\{^{1}H\}$ NMR spectrum of **3-Cl** (CD_2Cl_2, 99.4 MHz).

3.4. NMR Spectra of Cl–Ph_2Ge–Ph_2Ge–Cl

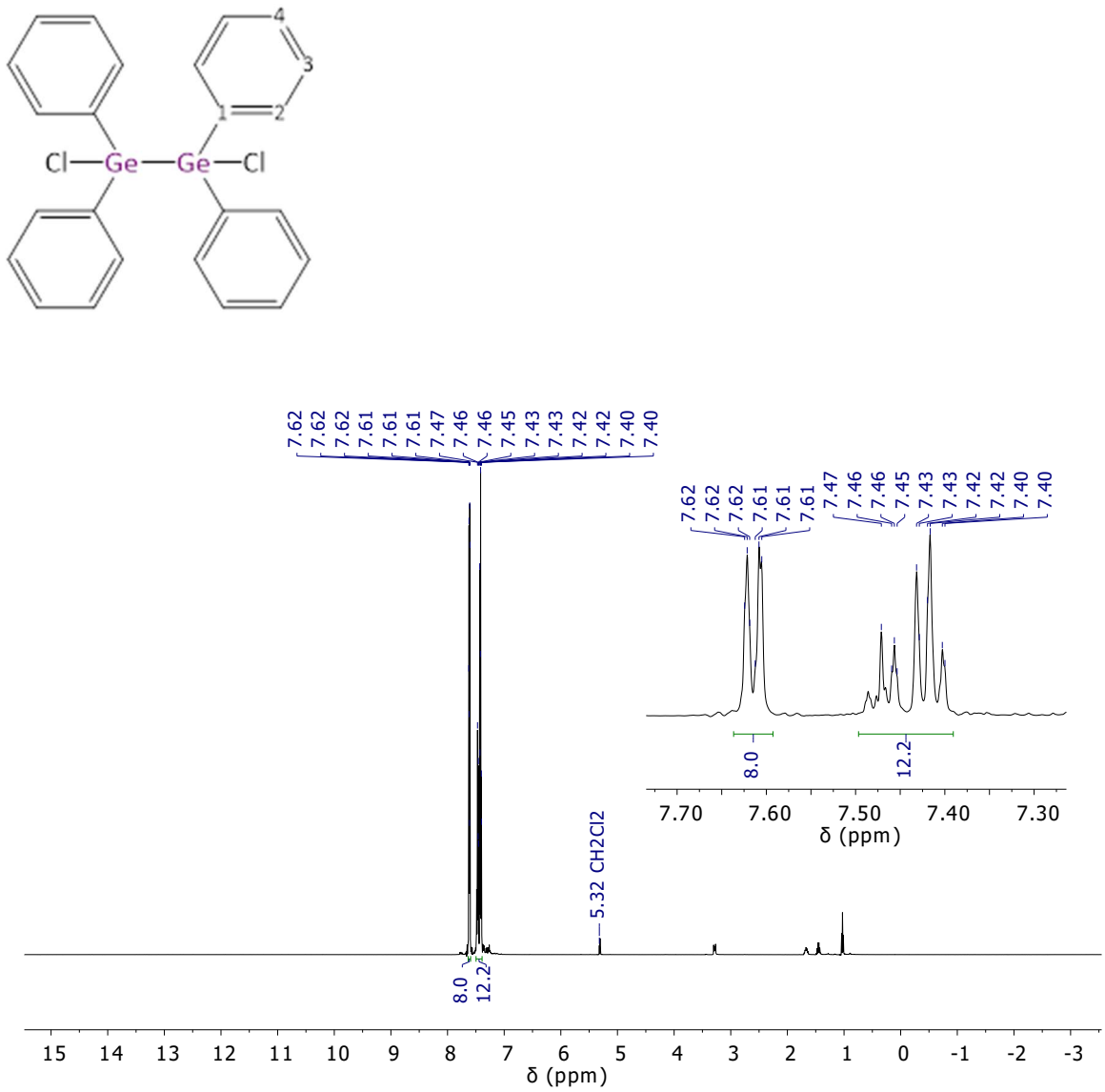

Figure S11. ^{1}H NMR spectrum (CD_2Cl_2, 500.2 MHz) of Cl–Ph_2Ge–Ph_2Ge–Cl containing small impurities of [*n*Bu_4N]Cl (cf. $^{13}C\{^{1}H\}$ NMR spectrum).

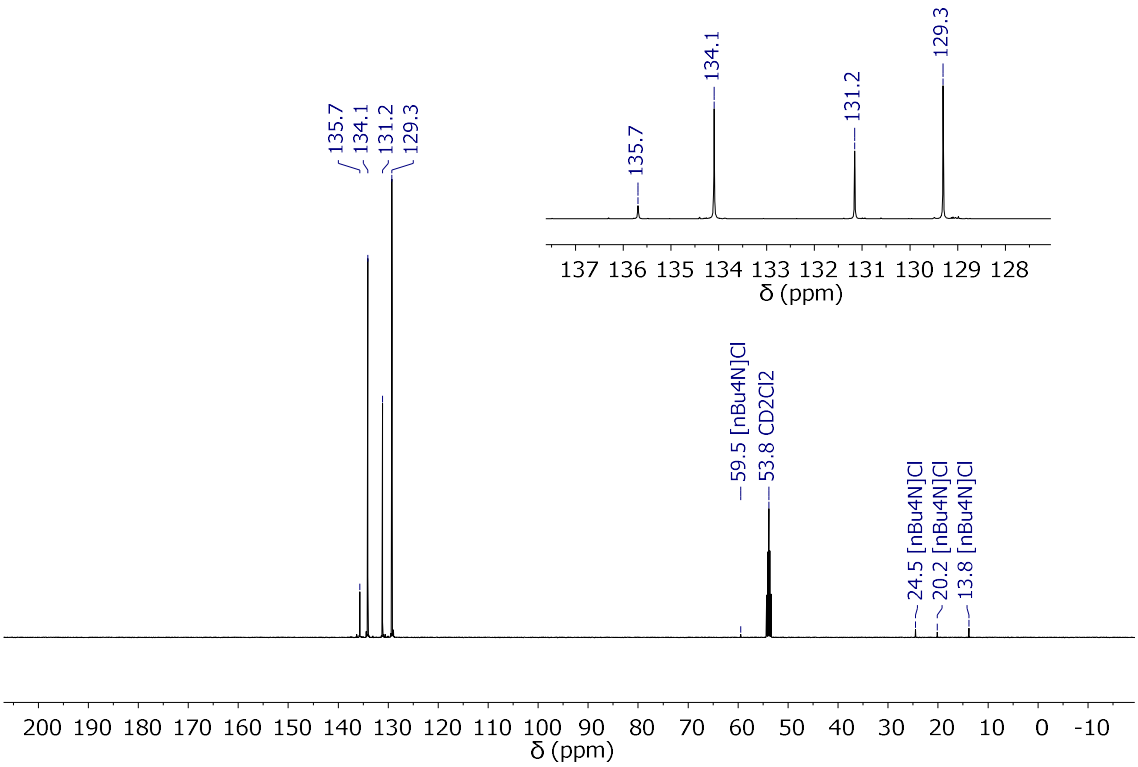

Figure S12. $^{13}C\{^{1}H\}$ NMR spectrum (CD_2Cl_2, 125.8 MHz) of Cl–Ph_2Ge–Ph_2Ge–Cl containing small impurities of [*n*Bu_4N]Cl.

3.5. NMR Spectra of 1-H

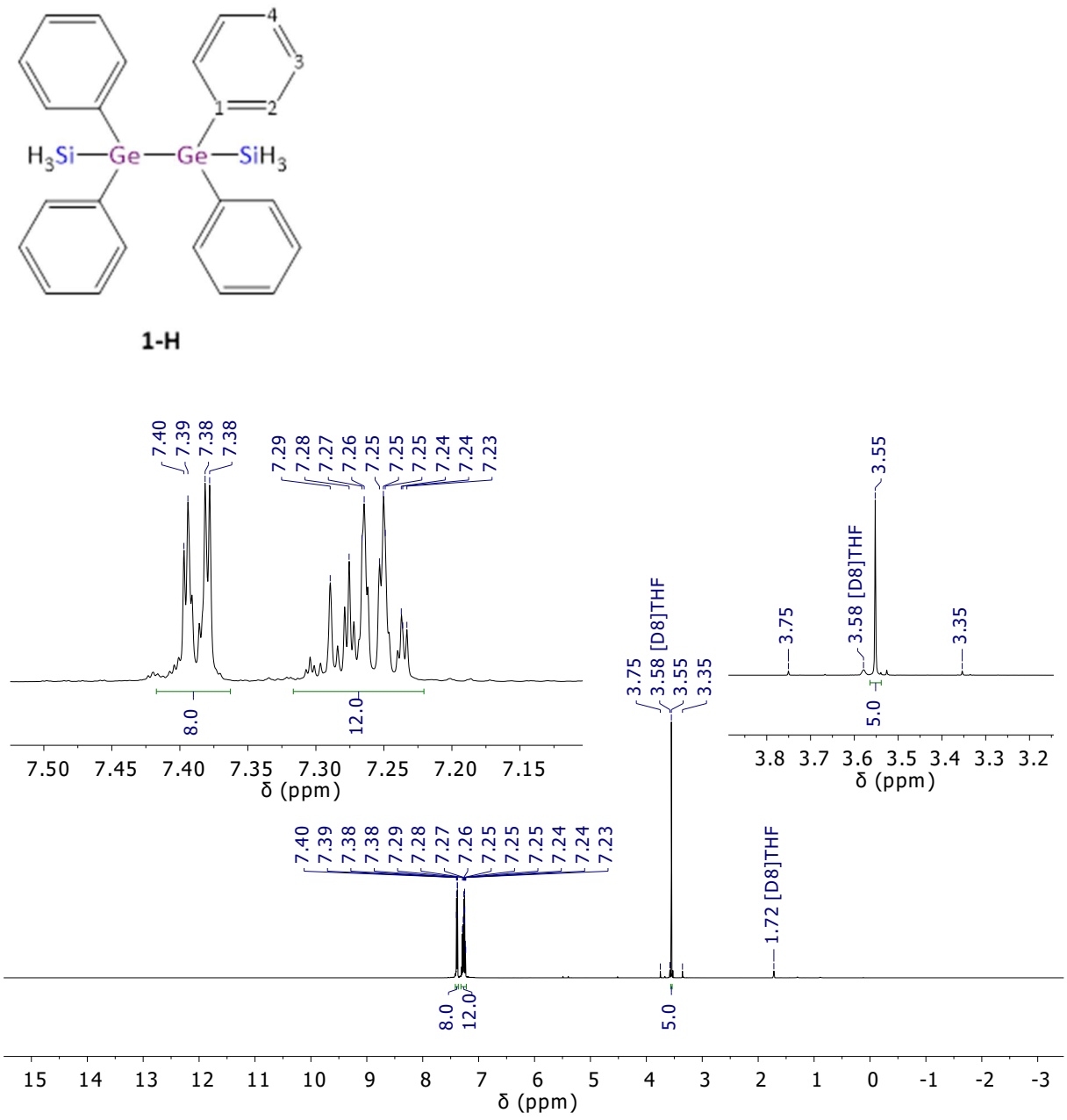

Figure S13. ^{1}H NMR spectrum of **1-H** ([D_8]THF, 500.2 MHz).

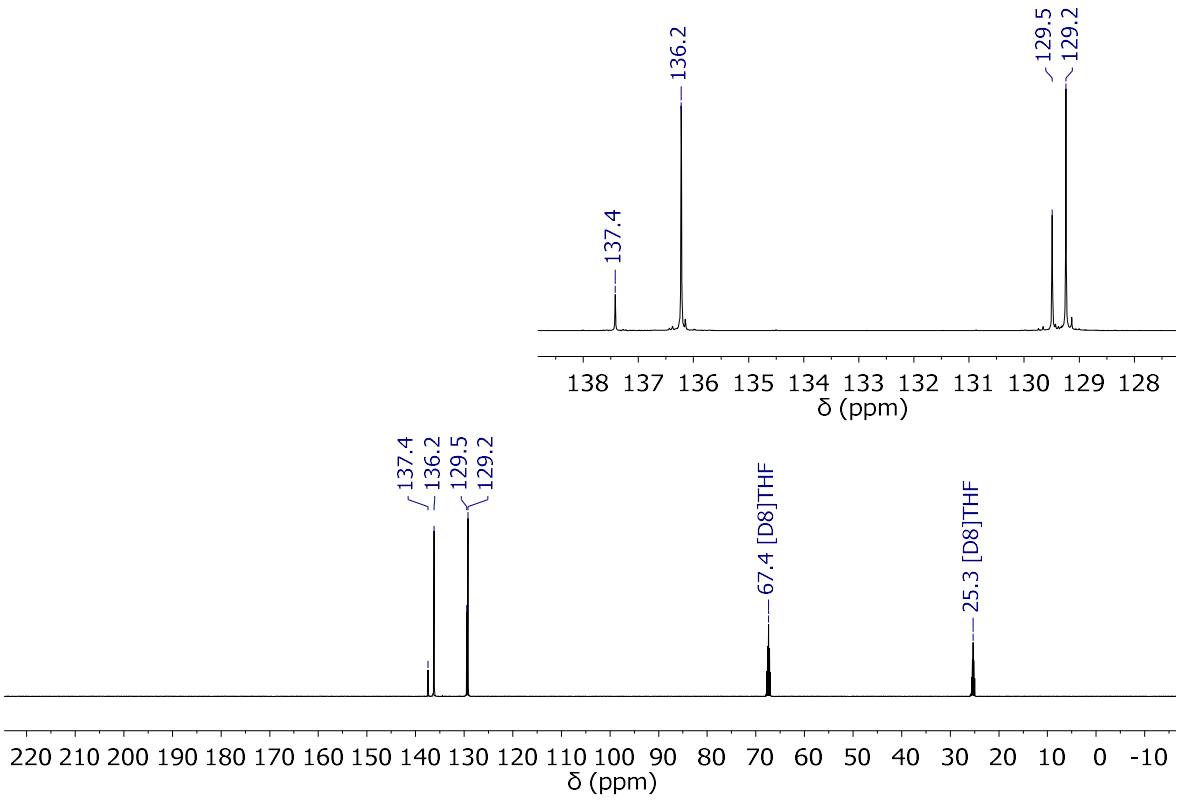

Figure S14. $^{13}C\{^{1}H\}$ NMR spectrum of **1-H** ([D8]THF, 125.8 MHz).

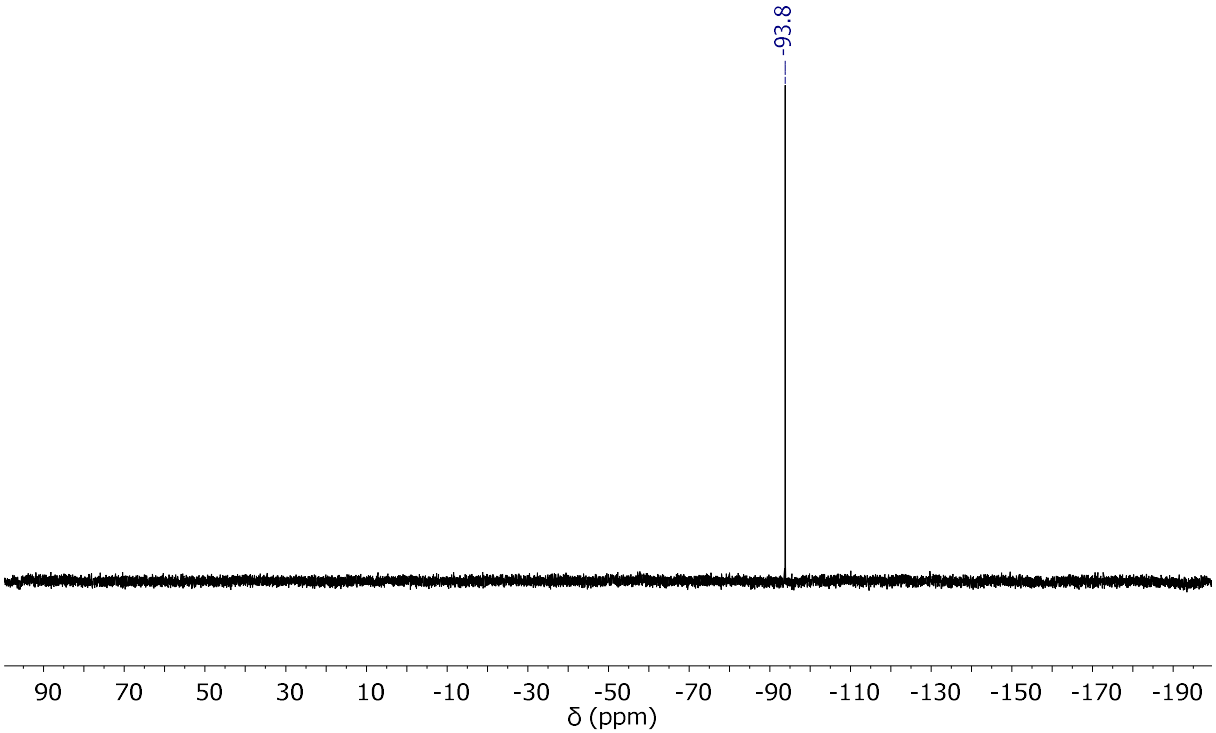

Figure S15. $^{29}Si\{^{1}H\}$ NMR spectrum of **1-H** ([D8]THF, 99.4 MHz).

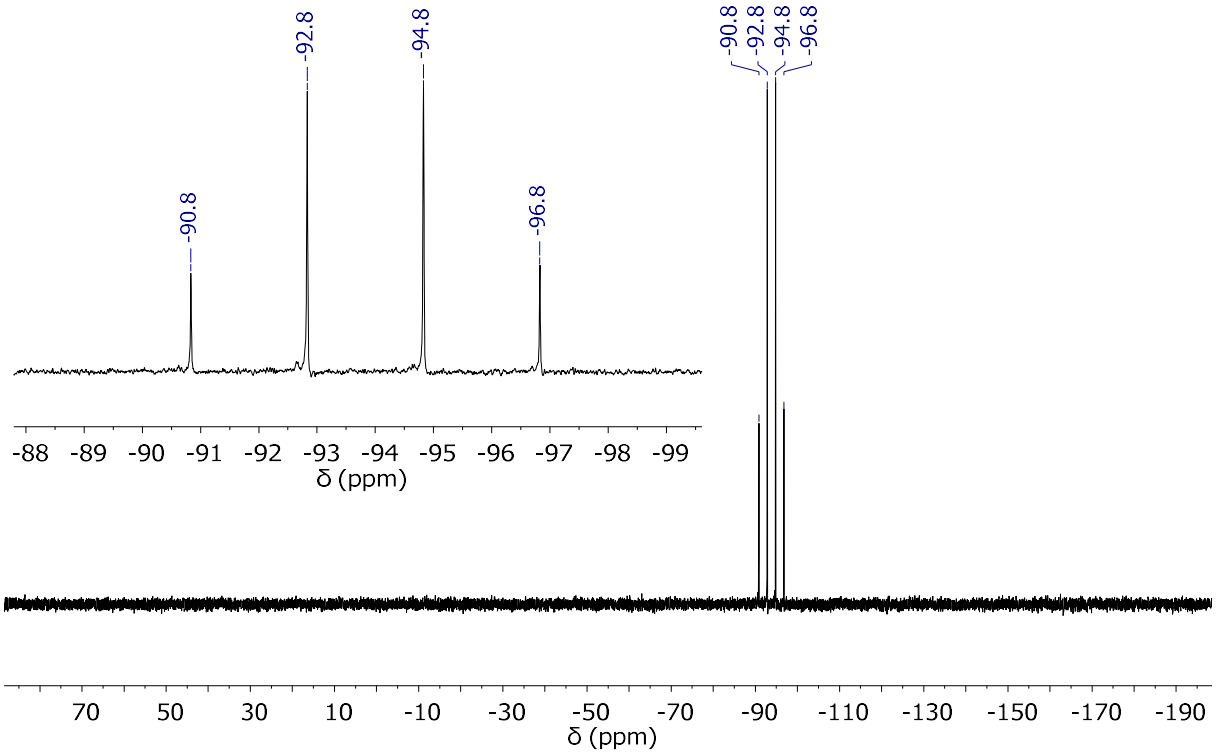

Figure S16. ^{29}Si NMR spectrum of **1-H** ([D_8]THF, 99.4 MHz).

3.6. NMR Spectra of 2-H

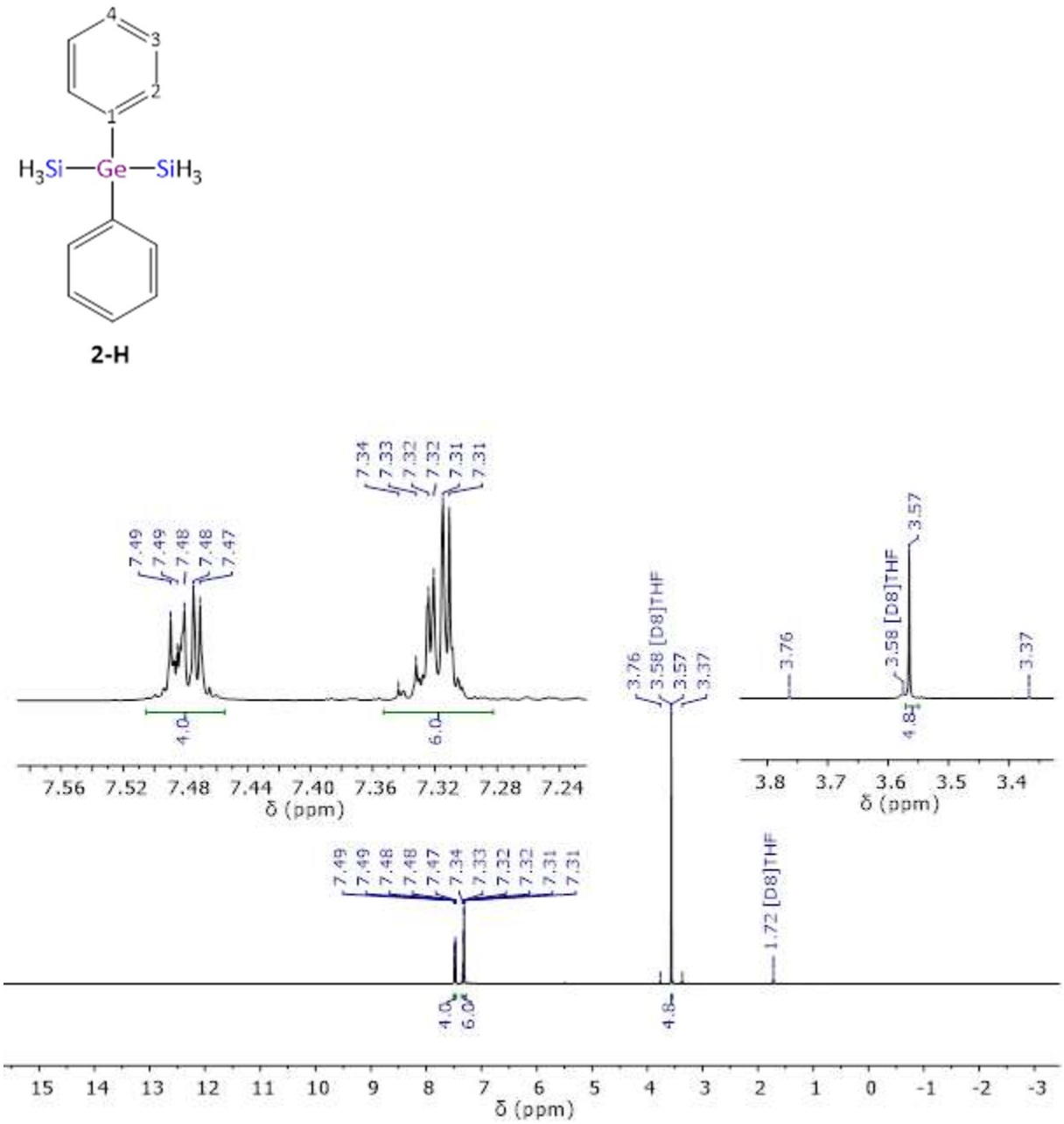

Figure S17. ^{1}H NMR spectrum of **2-H** ([D_8]THF, 500.2 MHz).

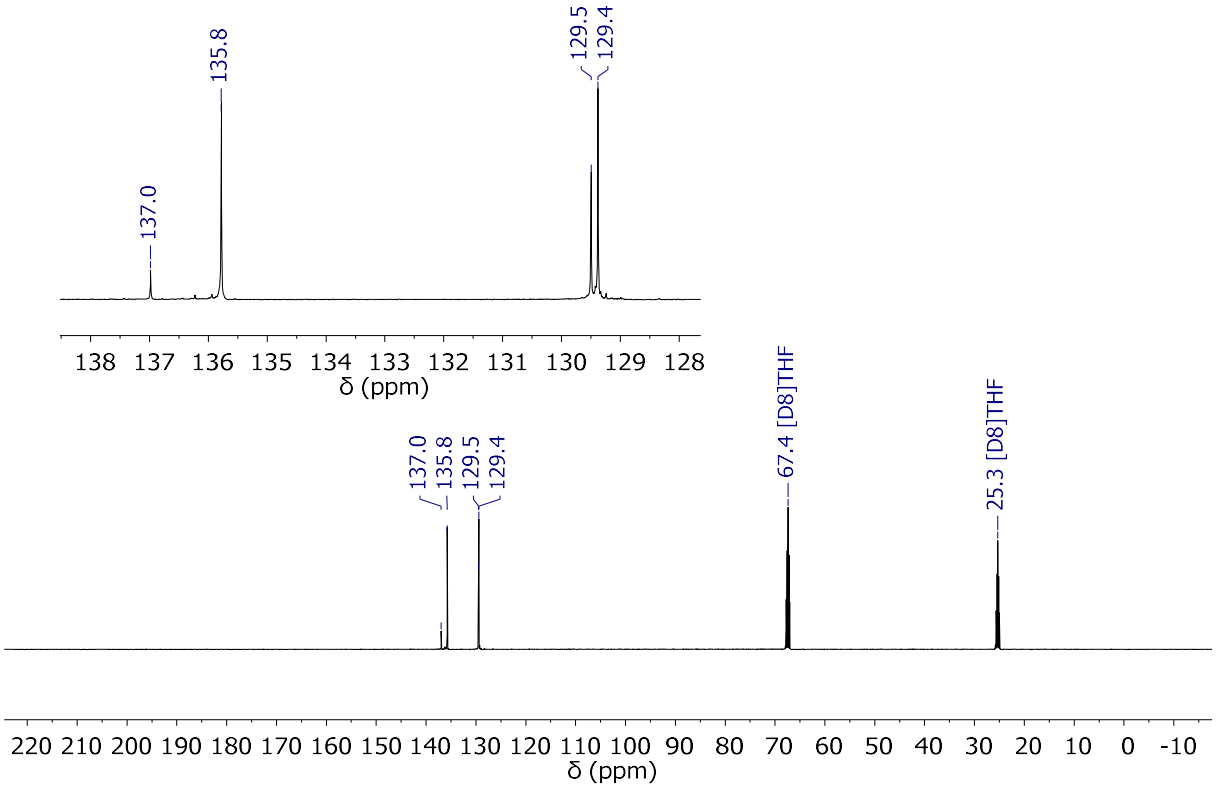

Figure S18. $^{13}C\{^{1}H\}$ NMR spectrum of **2-H** ([D8]THF, 125.8 MHz).

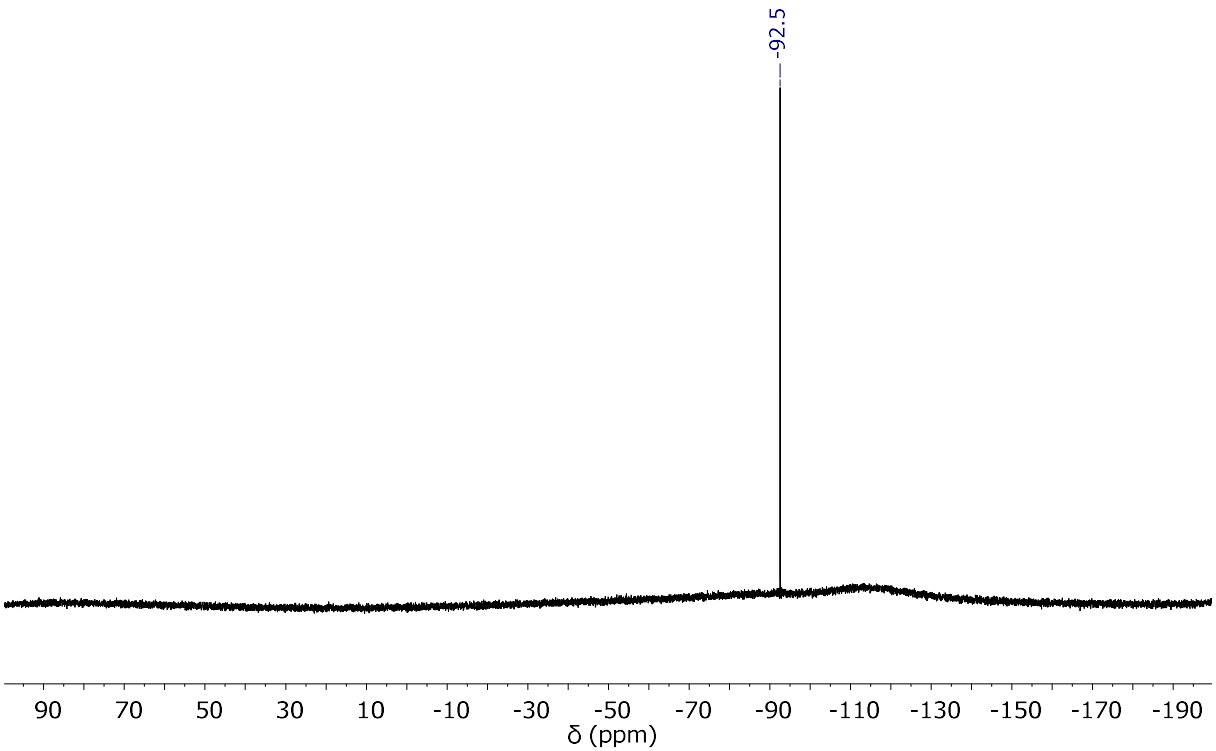

Figure S19. $^{29}Si\{^{1}H\}$+++ NMR spectrum of **2-H** ([D8]THF, 99.4 MHz).

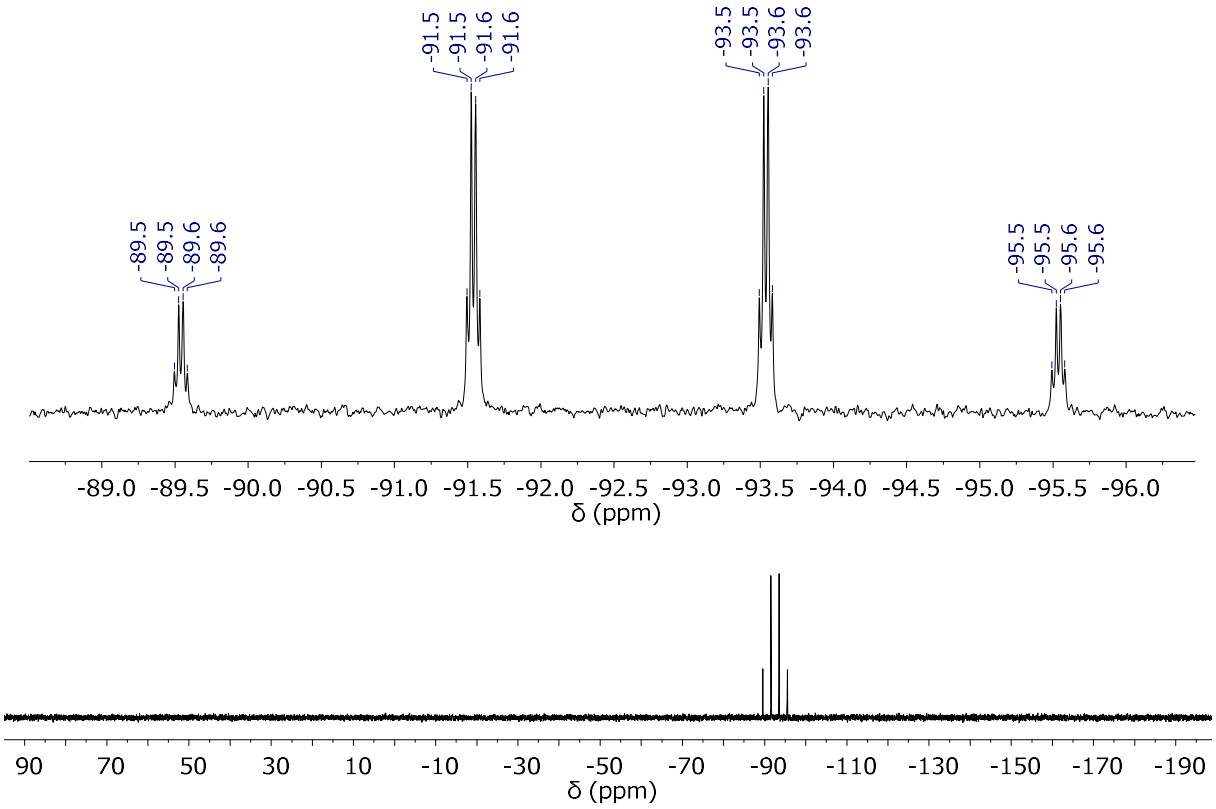

Figure S20. ^{29}Si NMR spectrum of **2-H** ([D_8]THF, 99.4 MHz).

3.7. NMR Spectra of 3-H

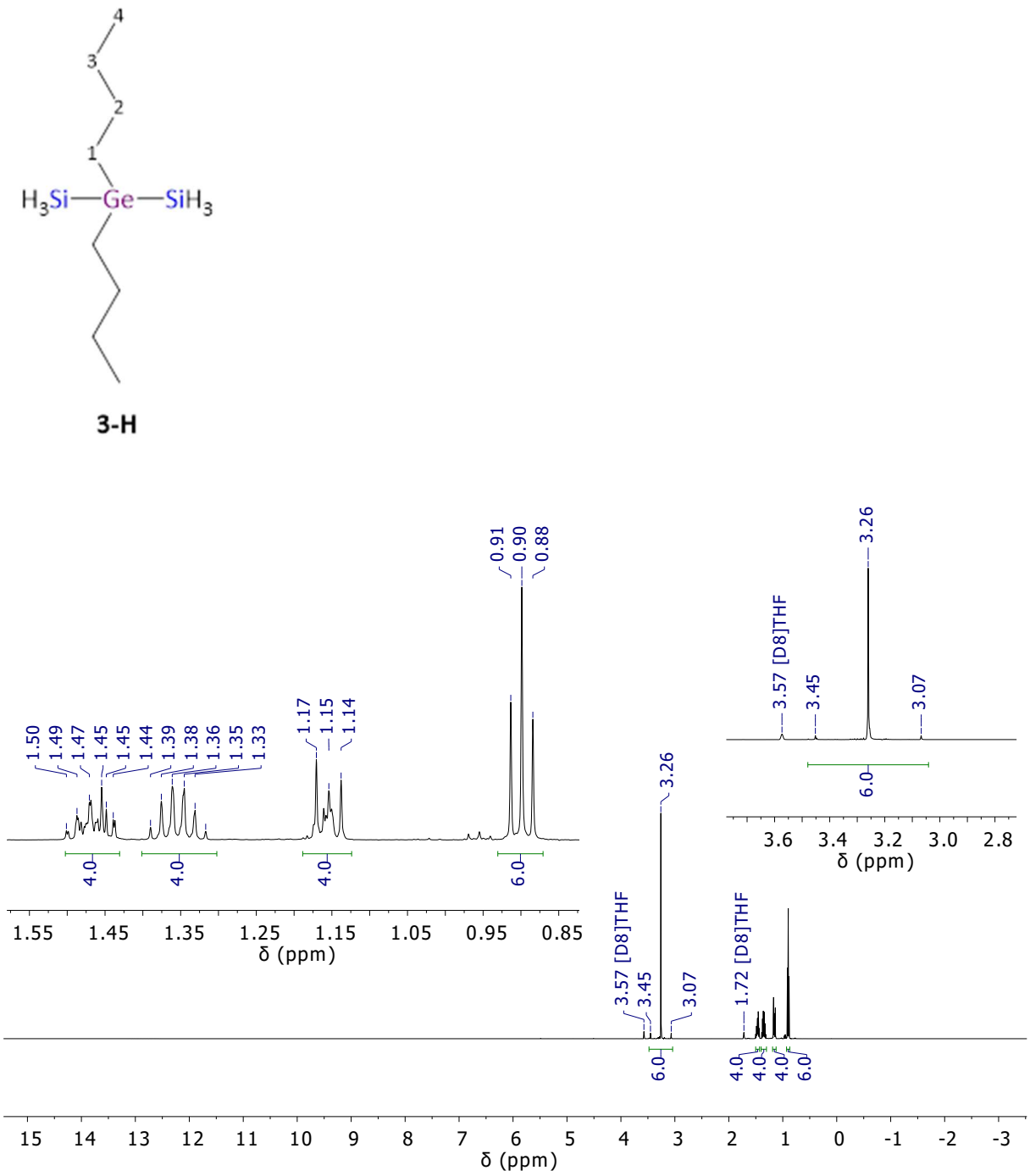

Figure S21. ^{1}H NMR spectrum of **3-H** ([D_8]THF, 500.2 MHz).

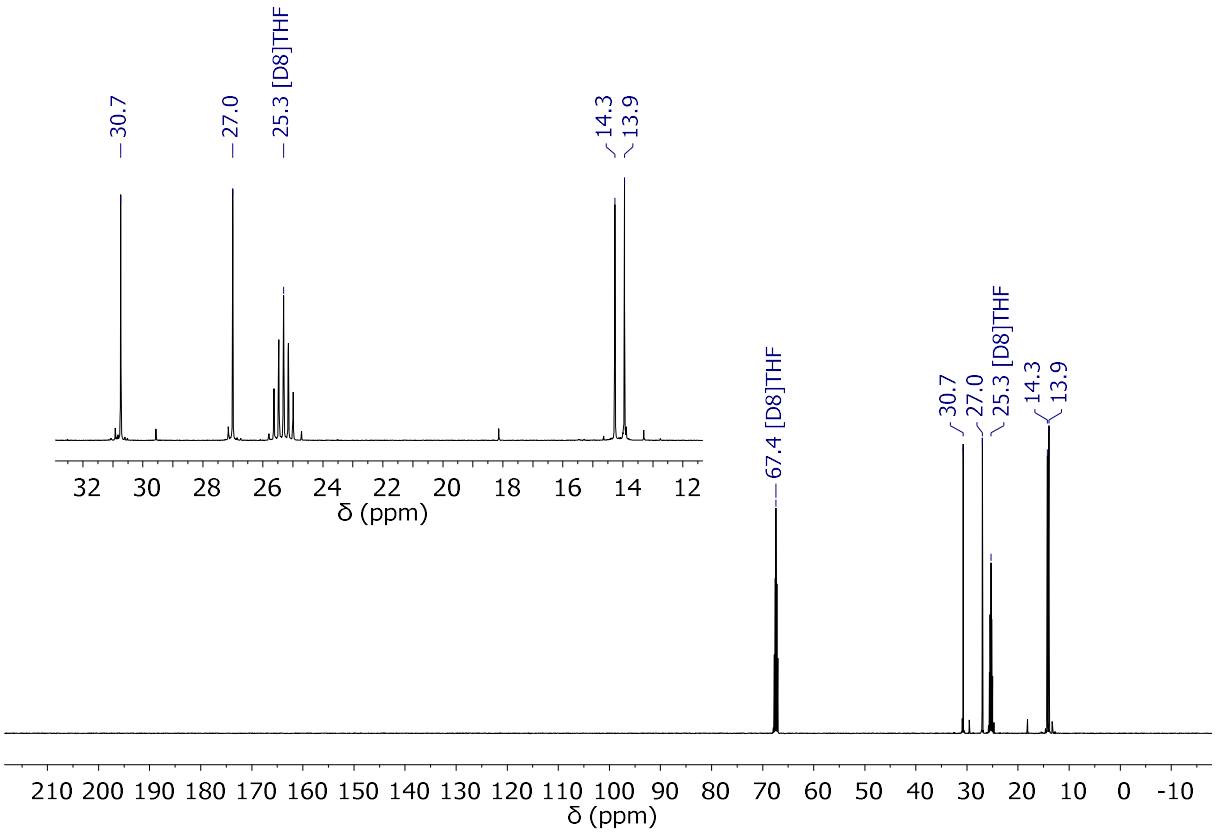

Figure S22. $^{13}C\{^{1}H\}$ NMR spectrum of **3-H** ([D_8]THF, 125.8 MHz).

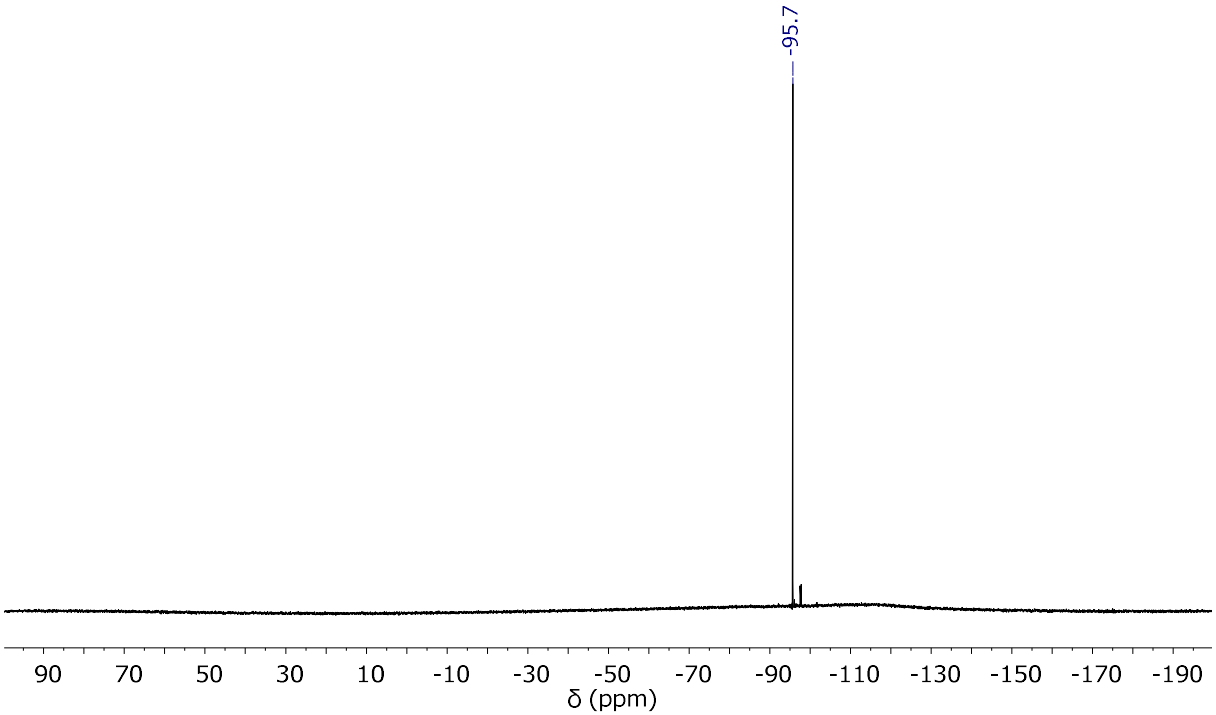

Figure S23. $^{29}Si\{^{1}H\}$ NMR spectrum of **3-H** ([D_8]THF, 99.4 MHz).

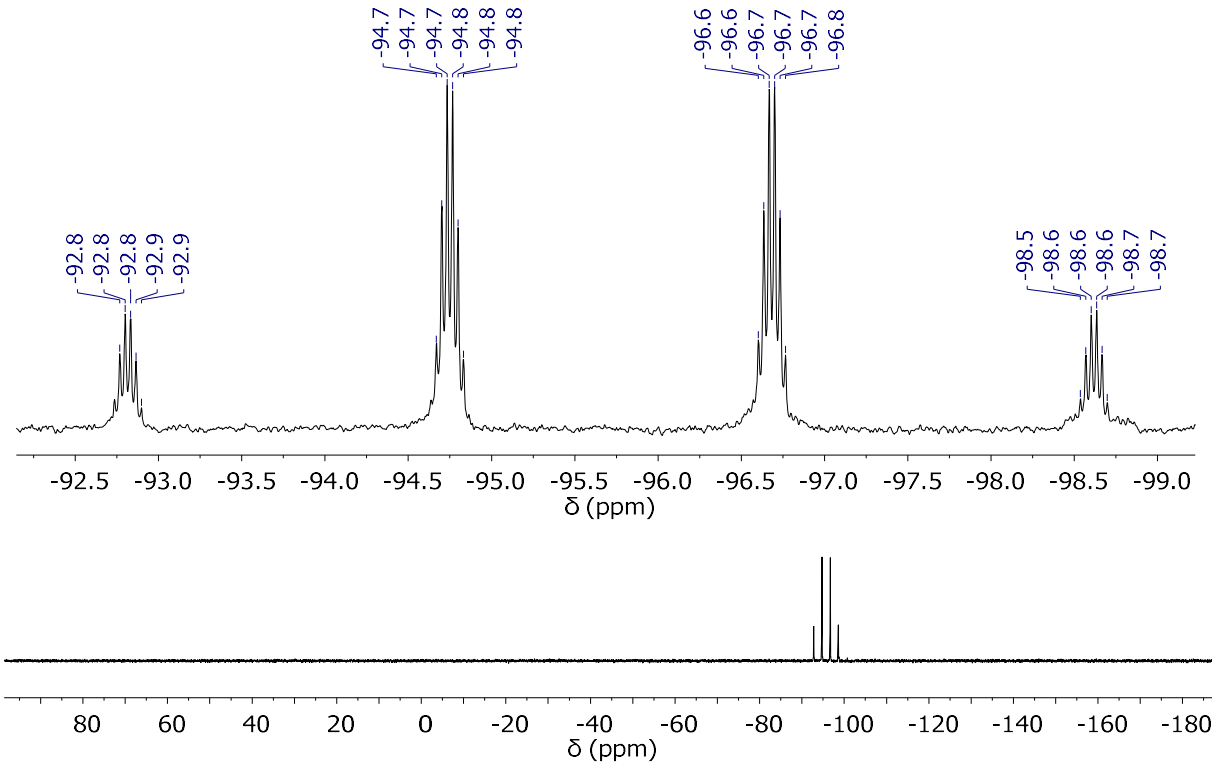

Figure S24. ^{29}Si NMR spectrum of **3-H** ([D_8]THF, 99.4 MHz).

4. Characterization of CVD Coatings

4.1. General Considerations

All reactions were carried out under an inert-gas atmosphere (dry argon or nitrogen) using standard Schlenk or glove-box techniques

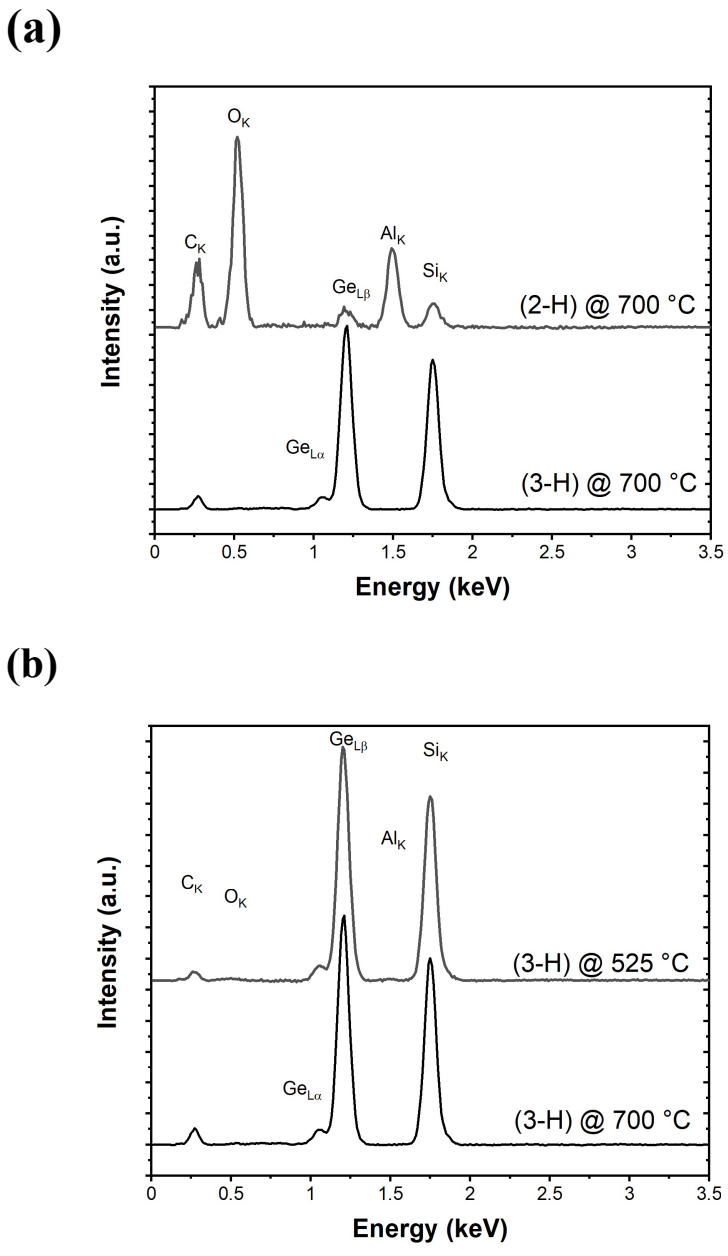

Figure S25. EDX spectra of (a) CVD films prepared using **2-H** and **3-H** at T_s=700 °C and (b) a comparison of the EDX spectra of $Si_{1-x}Ge_x$ films derived by using **3-H** at different substrate temperatures.

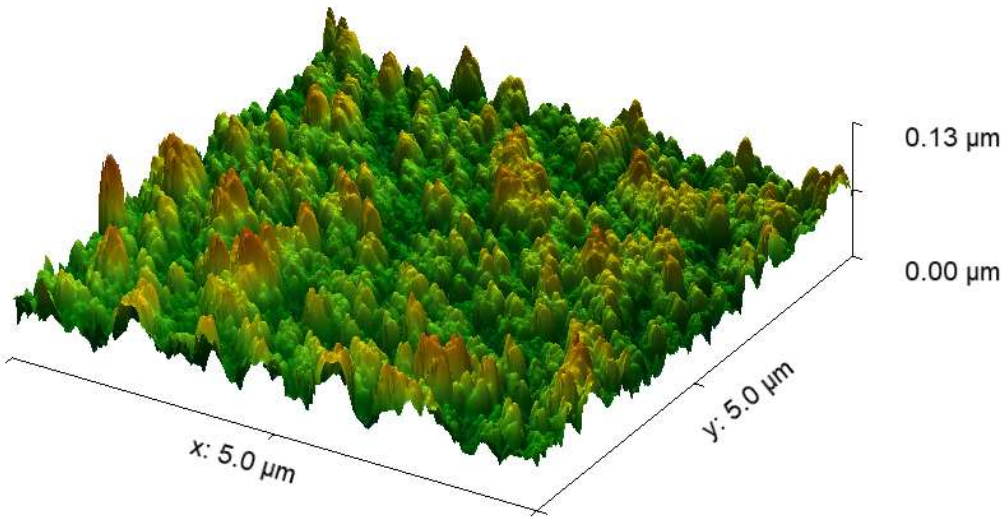

Figure S26. The AFM image of a $Si_{1-x}Ge_x$ deposit prepared at T_S=700 °C using **3-H** shows the formation of a smooth film without significant surface roughness.

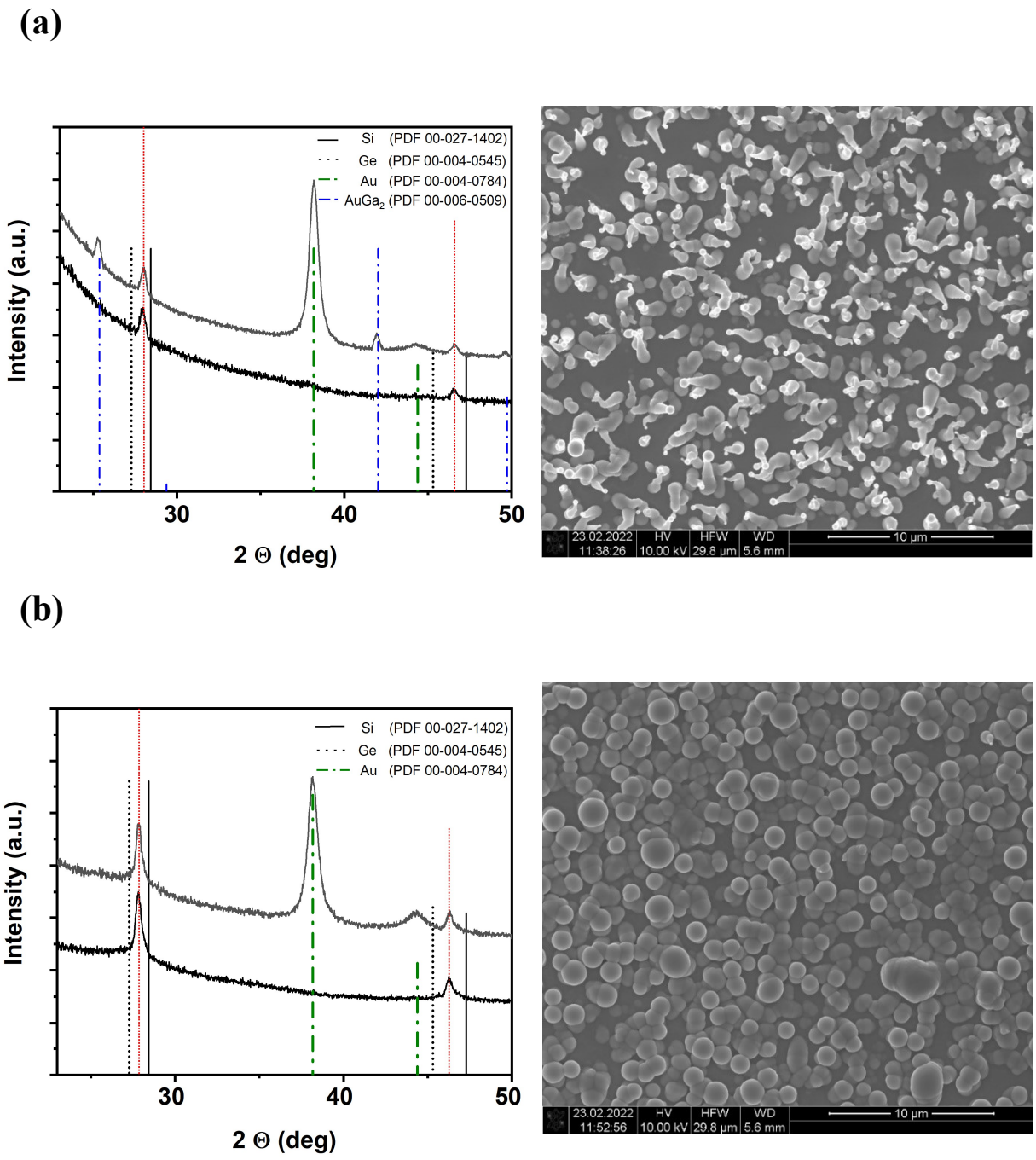

Figure S27. XRD and SEM images of Ga-supported crystallization of $Si_{1-x}Ge_x$ layers for (a) single Ga pulse and (b) three Ga pulses during the CVD using precursor **3-H** at T_S= 525 °C. Both films have been coated with Au post-growth to add a reference for XRD results. (a) represents Si:Ge ratio in the crystalline phase of 1.7 while in (b) merely 1.1 can be calculated by using Vegard's law.

5. References

1. Teichmann, J.; Kunkel, C.; Georg, I.; Moxter, M.; Santowski, T.; Bolte, M.; Lerner, H.-W.; Bade, S.; Wagner, M., Tris(trichlorosilyl)tetrelide Anions and a Comparative Study of Their Donor Qualities. *Chem. - Eur. J.* **2019,** *25*, 2740-2744.
2. Teichmann, J.; Wagner, M., Silicon chemistry in zero to three dimensions: from dichlorosilylene to silafullerane. *Chem. Commun.* **2018,** *54*, 1397-1412.
3. Satgé, J.; Rivière, P., Formation of the Germaniu-Germanium Bond by Reaction with Germyl-Metal Reagents. In *Inorganic Reactions and Methods*, J. J. Zuckerman; Hagen, A. P., Eds. VCH Publishers, Inc.: 1991; Vol. 9, pp 55-59.
4. Kraus, C. A.; Sherman, C. S., Preparation of Some Derivatives of Triphenylgermanium by Means of Sodium Triphenylgermanide. *J. Am. Chem. Soc.* **1933,** *55*, 4694-4697.
5. Cie, S. *X-AREA. Diffractometer control program system.*; Darmstadt, Germany, 2002.
6. Sheldrick, G., A short history of SHELX. *Acta Crystallogr., Sect. A* **2008,** *64*, 112-122.